Journal of Applied Polymer Science

Polythiophene nanoparticles in aqueous media

Kornelia Kadac, Jacek Nowaczyk
Faculty of Chemistry, Nicolaus Copernicus University in Toruń, Gagarina St. 7, Toruń 87-100, Poland
Correspondence to: J. Nowaczyk (E-mail: jacek.nowaczyk@chem.umk.pl)

ABSTRACT: The article presents the data concerning the synthesis of polythiophene (PTh) nanoparticles in aqueous medium applying emulsion polymerization. The synthetic method was studied in variety of combinations of initiator and surfactant. It was found that application of potassium peroxydisulfate (KPS) as initiator and sodium dodecyl sulfate (SDS) as the surfactant gives the best product yields. The structure, morphology, and physicochemical properties have been analyzed showing that the resulting latex have conducting film forming properties. Resulting polymers were characterized via fourier transform infrared spectroscopy (FTIR), scanning electron microscope (SEM), thermogravimetry-differential thermal analysis (TG-DTA), differential scanning calorimetry (DSC), and electrochemical methods [e.g. current–voltage characteristics (I–V), activation energy of electric conductivity, and doping processes]. A mechanism of the polymerization reaction is also discussed. © 2016 Wiley Periodicals, Inc. J. Appl. Polym. Sci. **2016**, *133*, 43495.

KEYWORDS: conducting polymers; electrochemistry; emulsion polymerization

Received 16 October 2015; accepted 31 January 2016
DOI: 10.1002/app.43495

INTRODUCTION

Conducting polymers, commonly known as synthetic metals, are a class of compounds that combine the characteristic attributes of typical plastics with the properties of electrically conductive materials. Furthermore, they have many advantageous features such as environmental and thermal stability, fair conductivity after doping and small band gaps. These properties of conducting polymers allow for a broad range of commercial applications as well as spur academic and industrial environments to design, synthesize, and study them.[1–4]

Application of aromatic monomers to synthesize conductive polymers has significantly improved their properties, exclusively the stability in ambient conditions. The polymers having aromatic systems incorporated in main chain exhibit high stability, relatively long π bonds conjugation extent, and low energy band gap. In this group of conducting polymers, one can mention: poly(*p*-phenylene) (PPP),[5] poly(*p*-phenylene vinylene) (PPV),[6] poly(*p*-phenylene ethynylene) (PPE),[7] polypyrrole (PPy),[8] polyaniline (PANI),[9] and polyfluorene (PF).[10] One of the best known group of conductive polymers is represented by polythiophene (PTh) and its derivatives.[11,12] Pure polythiophene (PTh) is inprocessable and insoluble in common solvents[13] due to strong intermolecular (interchain) interactions. The polymer obtained in organic solvents via organometallic coupling and chemical or electrochemical oxidative polymerization form dense packed polymer bundles. Consequently, it is hardly penetrable by any plasticizer of polymers. The common solution to overcome such difficulties consists of introduction of low molecular weight substances during polymer synthesis. It was recently proposed to synthesize polymers such as PTh from aqueous emulsion of monomer, in the form of latex.[14–19] Resulting polymer grains contain adsorbed surfactant molecules, which can act as plasticizers. Despite the content of additive, these conducting polymers can, after doping, reach the electrical conductivity characteristic for metals. Thus, the number of reports in the literature describing colloidal dispersions of conductive polymers is constantly growing and the process to obtain a conductive polymer emulsion by polymerization method becomes an important branch of material research.[20–28]

There are some reports of the emulsion polymerization of aniline and 3,4-ethylenedioxythiophene (EDOT) in the literature.[20–28] However, similar works concerning polythiophene (PTh) are seldom. One can find reports concerning studies of structure, morphology or thermal stability of PTh.[14–19] These articles describe the reactions that usually use ion Fe^{3+}, e.g. $FeCl_3$, as the initiator.[11,15,17,18,29,30] The systematic study of the emulsion polymerization of thiophene in various conditions was not published yet. This article is the first approach to such goal. There is large number of thick books written about the emulsions and chemical processes in colloidal systems, however, it occur that in any particular case, emulsion polymerization seems to be more art than science. In chemical processes taking place in colloidal state, surfactants plays a key role by adsorbing to the surface of dispersed phase and lowering its surface energy. In the emulsion polymerization, this aspect is more important because it influences the kinetics of polymerization reaction and control the size

Table I. Details of Polythiophenes Polymerization Conditions and Achieved Yields

	$C_{Initiator}$ (mol dm^{-3})		$C_{Emulsifier}$ (mol dm^{-3})			
Entry	KPS		SDS		The reaction time (h)	Yield (%)
1	0.06		0.35		2.5	15
2	0.06		0.35		5	73
3	0.06		0.35		10	46
	APS		CTAB	TEA		
4	0.72		0.09	0.53	24	43
5	0.72		0.13	0.72	24	60
6	0.72		0.13	0.85	24	32
7	0.72		0.13	0.90	24	28
8	0.72		0.26	0.72	24	38
9	0.80		0.13	0.72	24	35
10	0.72		0.13	0.72	48	62
	$Fe(OTs)_3\times 6H_2O$	H_2O_2	DBSA			
11	0.05	0.93	0.08		24	21
12	0.05	0.93	0.08		48	22

KPS, potassium peroxodisulfate; SDS, sodium dodecyl sulfate; APS, ammonium persulfate; CTAB, cetyltrimethylammonium bromide; TEA, triethanolamine; DBSA, dodecylbenzene sulfonic acid.

and shape of the product particles. In present work, we report the results of thiophene polymerization in presence of tree different ionic surfactants. Cetyltrimethylammonium bromide (CTAB) is a cationic surfactant with abilities to break the water phase structure, commonly used in synthesis of nanoparticles. In water, it forms micelles of average size about 6 nm. The other two are anionic surfactants with different structure and properties; sodium dodecyl sulfate (SDS) is a common surfactant widely used in laboratory practice and industry, and dodecylbenzene sulfonic acid (DBSA) is often reported in synthesis of conjugated polymers. The former is known to form micelles of average diameter about 4.5 nm. The latter is acidic surfactant capable to form stable micelles at very low pH, the micelles average diameter in water ranges from 5.7 to 7.5 nm and strongly depend on the concentration; it is also known that DBSA is effective dopant of conducting polymers.

In this article, we describe the polymerization of thiophene by chemical oxidation in the aqueous environment. The process complexity involves the choice of adequate oxidizing agent as well as surfactants and emulsion stabilizers. The high oxidation potential of thiophene limits the range of adequate oxidizing agents. In present article, we show results of polymerization of thiophene carried out in systems containing various initiators and emulsifiers. Further, we compare our data with previously published results of iron (III) initiated polymerization.

EXPERIMENTAL

Materials

Monomers: thiophene (≥99%) was purchased from Sigma-Aldrich Chemie GmbH, Schnelldorf, Germany. The chemical was freshly distilled prior to use. Potassium peroxodisulfate (KPS, ≥99%), ammonium persulfate (APS, ≥99%), iron (III) *p*-toluenesulfonate hexahydrate (technical grade) and sodium dodecyl sulfate (SDS, ≥99%), cetyltrimethylammonium bromide (CTAB, ≥99%), and triethanolamine (TEA, ≥99%) were also obtained from Sigma-Aldrich Chemie GmbH, Schnelldorf, Germany. Dodecylbenzene sulfonic acid was purchased from Acros Organics, Geel, Belgium. Hydrogen peroxide solution (30%) and hydrochloric acid (37%) were obtained from Avantor Performance Materials Poland S.A., Gliwice, Poland. Tetrabutylammonium tetrafluoroborate (99%) and ferrocene (98%) were purchased from Sigma-Aldrich Chemie GmbH, Schnelldorf, Germany. Acetonitrile (99.5%) was obtained from Avantor Performance Materials Poland. These reagents were used without further purification. Deionized water was used throughout the experiments.

Synthesis

Polythiophene was obtained according to different methods as it is described below. The detailed conditions and reagents concentrations are given in Table I.

Polymer I. The polymer was prepared by emulsion polymerization. Thiophene (4 cm^3, 50 mmol) and sodium dodecyl sulfate (SDS) (25 mmol) were dissolved in deionized water (30 cm^3, 1660 mmol) in a round flask. The solution was placed under ultrasonic for 10 min. A uniform, milk-like dispersion was formed. The mixture was heated with stirring to 70 °C. Potassium peroxodisulfate (4 mmol) was dissolved in 40 cm^3 of deionized water (2213 mmol) and added dropwise into preheated emulsion of monomer in water within 0.5 h. The mixture was continuously mixed and kept in elevated temperature 70 °C to obtain a stable dispersion with dark brown color. The polymerization was then terminated by pouring the emulsion into methanol (500 cm^3) to precipitate polythiophene. The resulting precipitate was collected by filtration, washed thoroughly with methanol (150 cm^3) and then with deionized water. The powder was dried in a vacuum oven at 50 °C for 48 h.

Polymer II. Cetyltrimethylammonium bromide (CTAB) from 5 to 13 mmol, triethanolamine (TEA) from 26 to 45 mmol, and

thiophene (2.5 cm^3, 31 mmol) were dissolved in 30 cm^3 of deionized water (1660 mmol). The mixture was placed in ultrasonic bath for 10 min. In a separate beaker, initiator solution was prepared by dissolution of ammonium persulfate (APS) from 36 to 40 mmol in deionized water (20 cm^3, 1107 mmol). The reactant mixture was stirred and heated continuously at 70 °C. The solution of initiator was added dropwise into the first solution. The precipitate was collected by filtration. The brown powder was filtered, purified, and drained as above.

Polymer III. Dodecylbenzene sulfonic acid (DBSA) (6 mmol) and thiophene (2.5cm^3, 31 mmol) were dissolved in deionized water (40 cm^3, 2213 mmol). The solution was stirred for 30 min. Iron (III) *p*-toluenesulfonate hexahydrate (4 mmol) was dissolved in deionized water (30 cm^3, 1660 mmol). It was added into the first solution. After 1 h, hydrochloric acid (1 cm^3, 33 mmol) was dripped into the reaction system. Then, hydrogen peroxide solution (2 cm^3, 65 mmol) was added into the reactant mixture. The mixture was stirred and heated at 70 °C. Final procedures were performed as above.

Characterization

FTIR spectroscopy was applied for definition of the polythiophene structure by showing the bands related to oscillations of specific functional groups in the molecules. Spectrum was registered on a Thermo Scientific Nicolet iS10 FTIR spectrometer in radiation frequencies range 400–4000 cm^{-1}. The analyzed sample was blended with dry potassium bromide (KBr) at mass ratio 1 : 100, homogenized in a ball mill, and pressed to the form of transparent pellets using hydraulic press. The X-ray diffraction (XRD) study was performed using HZG-4/A-2 apparatus. Samples in form of powders were subjected to X-ray radiation in the angular range of 10–30. The morphology of the samples in the form of free powder was examined using the scanning electron microscope (SEM) Quanta 3D FEG. Thermogravimetric analysis TG-DTA was studied using Simultaneous TGA-DTA Thermal Analysis TA Instruments SDT type. The samples thermal properties were measured in temperature range 20–600 °C with heating rate of 10 °C min^{-1} in the inner gas atmosphere (nitrogen). Differential scanning colorimetry DSC was conducted using the apparatus PL DSC (Polymer Laboratories, Epson, UK) in nitrogen environment at a temperature from 25 to 200 °C and heating rate of 10 °C min^{-1}.

To determine the electrochemical properties of the polymer, samples pressed powder pellets were obtained by pressing polymer powder in the laboratory press under pressure 70 bar. Gold contacts were evaporated in vacuum. The thicknesses of the prepared structures were measured.

The cyclic voltammetry (CV) measurements were carried out using three electrode system consisting of polythiophene in form of pellets with one gold contact as the working electrode, the Ag/AgCl reference electrode, and Pt counter electrode. The analyses were conducted without the presence of monomer in deaerated acetonitrile containing Bu_4NBF_4 (0.1 mol dm^{-3}) and ferrocene (1×10^{-4} mol dm^{-3}) as the redox indicator.

The current–voltage characteristics (I–V) and volume dc-conductivity (σ_{dc}) of polymer was studied on samples in the form of pressed pellets with two gold contacts. Measurements were made applying two point probe electrometer. The pellets were analyzed at three different temperatures 298, 308, and 318 K. The activation energy of electric conductivity of the materials in the native state was measured in the systems similar lab setup according to following procedure. The pellets were placed in a thermostatic chamber and the temperature was increased from 293 to 473 K with constant rate of 2K min^{-1}. Constant voltage 25 V was applied to gold contacts and fluctuations of dc-current was recorded. Kinetics of iodine doping was studied in the vessel consist of the thermostated iodine source and two electrode electrometer terminal. The tests were performed at 343 K and I_2 partial pressure 10 Torr.

RESULTS AND DISCUSSION

The Polymerization Conditions and Mechanism of the Process

The emulsion polymerization was commercialized in 1930s, and since then it has been widely used and improved. It is a common large-scale method used to produce environmentally friendly latex products. Emulsion polymerization is usually coupled with the radical polymerization, particularly with heterogeneous free radical polymerization. The first step of this process is emulsification of hydrophobic monomer in water mediated by oil-in-water emulsifier. The next stage is initiation reaction with either a water-soluble initiator or oil-soluble initiator. The reaction is followed by the propagation reaction, which is the polymer chain growth step of the process. The compatibility between polymer growing inside the oil droplet and the water continuous phase is rather poor. The oil–water interface area increase substantially while the polymer particle grows in size during propagation step. Consequently, effective stabilizer such as surfactant or protective colloid is necessary to prevent the coagulation of latex particles. It makes the emulsion polymerization quite complex process and requires systematic studies of the influence of each component of the system on the product and process yield. In the course of this study, we have tested different initiator–emulsifier couples to determine their influence on the polymerization yield and product properties. Table I shows details of tested initiator–emulsifier systems and yields of the process. To compare the data with these previously reported in the literature, one of the systems (Polymer 2) was obtained in similar way as it was previously described giving reaction yield 75%.[14] The process was repeated in our lab several times giving the best yield about 62%. Comparing with other conditions tested in recent study, conditions in synthetic route Polymer was not among the best results. The best results obtained in this work concern the system consist of potassium peroxydisulfate (KPS) as initiator and sodium dodecyl sulfate as the surfactant (Polymer I) giving yield about 73%. Therefore, further more detailed research was dedicated to this system.

Literature data indicate that the redox potential of persulfate ions (initiators: potassium persulfate and ammonium persulfate) is 2.01 V and of Fe^{3+}/Fe^{2+} is 0.771 V,[31,32] while oxidation potential of the monomer is about 2.0 V.[33] According to this, one can assume that APS and KPS are more effective oxidants than that with Fe^{3+}. According to the data in Table I, the best yield of PTh is obtained in reaction using KPS and SDS at 5 h. Effect of SDS concentration on the reaction yield is discussed separately.

Aside of the initiator, in emulsion polymerization, surfactants and stabilizers are of vital importance to the process. One of the

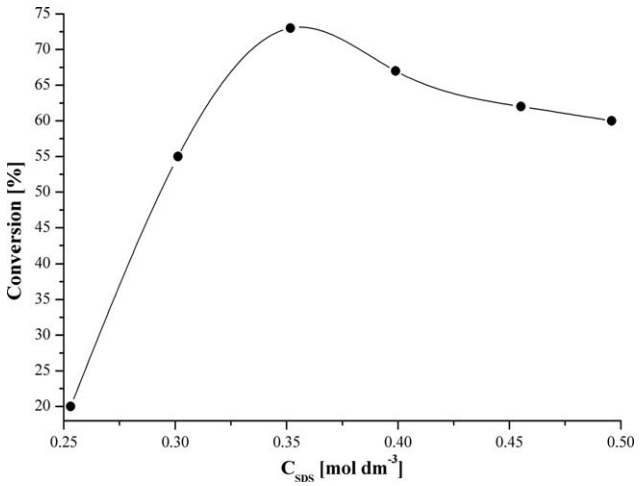

Figure 1. Effect of emulsifier (SDS) on polymerization yield of thiophene.

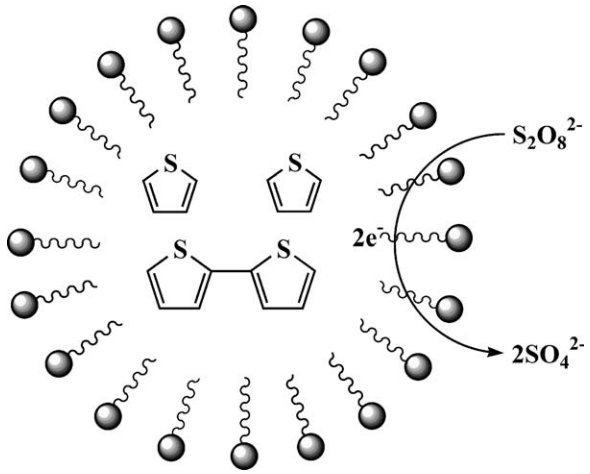

Figure 2. The scheme of polythiophene formation in micelle.

crucial factors controlling the process conditions is the surfactant concentration. The reaction system consists of hydrophobic monomer dispersed in the aqueous continuous phase containing oxidizing agent. Large oil–water interfacial area is obtained by fine dispersion of the oil phase. The emulsifying agents play important role in stabilization of the interfacial surface. In Figure 1, the effects of the SDS concentration on the reaction yield is shown. The polymerization yield increase with concentration of emulsifier up to 0.35 mol dm^{-3}; further increase of surfactant concentrations lead to slight decrease of reaction yield. It can be explained by the influence of emulsifier on micelles size. Increase of surfactant concentration results in decrease of micelles size. Emulsion polymerization, though is strongly controlled by micelles size. Large micelles suffer from hindered diffusion of initiator from aqueous continuous phase, however small size micelles contain limited content of monomer. In the former case, the concentration of initiator inside micelles is low and polymerization proceeds slowly; in the latter case, there is too little of monomer inside of small micelles to yield high molecular weight product. It was found that the optimal concentration of SDS in reaction mixture is about 0.35 mol dm^{-3}. During the course of the reaction, the solution change from colorless to brown and the dark brown powder precipitates.

The first step of the process is mediated by the surfactant formation of micelles containing monomer phase (Figure 2). The monomer is oxidized by the persulfate anions diffusing into micelles from aqueous continuous phase. The monomer inside micelle is transformed into adequate radical cation. In the following step, two radical cations couple to form the dihydro dimeric dication, which spontaneously undergoes deprotonation and aromatization. Finally, the dimer is formed. In the next step, the dimer is oxidized to radical cation and via coupling with monomeric or oligomeric radical cation participates in the chain growing reaction. The consequence of main chain elongation is the darkening of the reaction mixture. In the process, persulfate anions are reduced to sulfate anions (Figure 3).

pH Stability Tests – Polymerization I

The pH sample I was tested in regular time intervals (0.5 h) at room temperature. Figure 4 indicates that pH gradually decreases with time to reach the saturation level (at pH = 1) after 2.5 h. Since pH decrease originates in increase of H^+ concentration, recorded data supports the proposed reaction mechanism in which H^+ ions are the side product of the thiophene rings coupling.

FTIR Spectroscopy

The FTIR spectrum of polymer (Polymer I) was recorded and analyzed (Figure 5). It gives a set of important information about the structure of resulting polymer and proves that the main product is polythiophene. The characteristic C–H stretching vibration peak at thiophene ring was found at 3103 cm^{-1}. In the range of 2800–3000 cm^{-1}, it can be found typical formation of aliphatic C–H stretching vibrations that can be assigned to the aliphatic tail of the SDS. The intensity of these peaks is much higher than the intensity of the band at 3103 cm^{-1}, however, it does not imply high concentration of surfactant because the strength of bond oscillator for aliphatic C–H is several folds

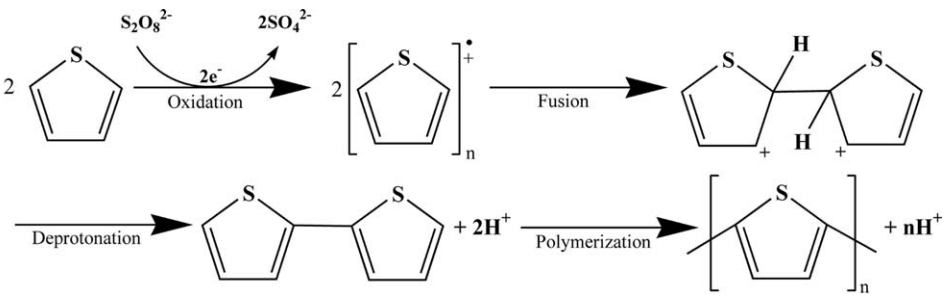

Figure 3. The mechanism of thiophene polymerization mediated by peroxodisulfates.

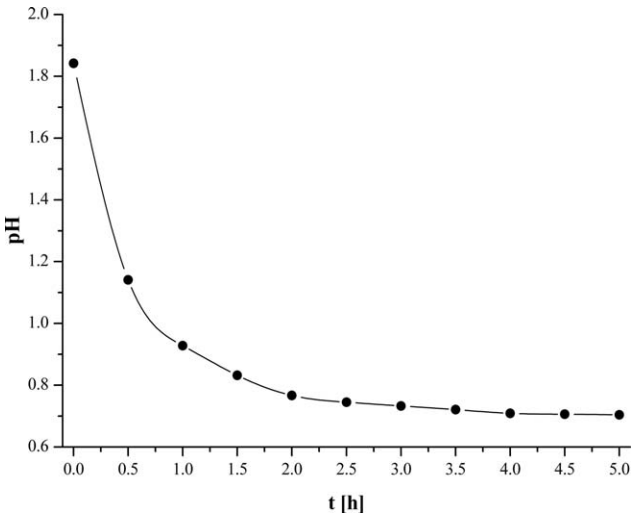

Figure 4. Representative plot of pH vs. polymerization time.

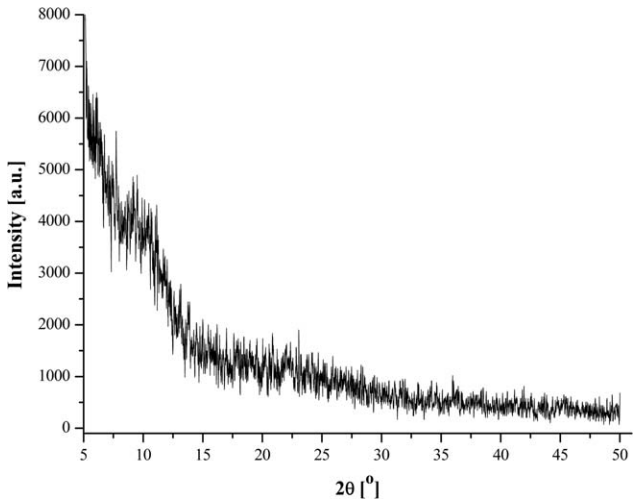

Figure 6. XRD diffractogram of Polymer I.

greater than that of aromatic C–H. The characteristic vibration band of SDS occurs at 1466 cm^{-1} and intensity of this band has low intensity indicating low content of the SDS in product. The bands at 1683, 1466, and 1411 cm^{-1} can be assigned to different modes of C=C stretching vibrations in the thiophene ring.[16,29] Absorption peak at 1261 cm^{-1} refers to in-plane stretching of C–H. The peaks at 1177, 1116, and 991 cm^{-1} are assigned to variety of bending modes of C–H. The band at 802 cm^{-1} is specific for C–S stretching vibration. The band at 704 cm^{-1} is caused by C–H out-of-plane bending vibration absorption. The peak at 616 cm^{-1} is representative for the ring deformation of C=S=C moiety in polymer chain. The FTIR spectrum of polymerization product shows that the characteristic absorption bands of PTh are analogous to those observed in polymer obtained by standard methods.[18,19,34] The spectra recorded for Polymer II and III are similar.

X-ray Diffraction Studies (XRD)

X-ray diffraction (XRD) chart taken for Polymer I is shown in the Figure 6. The XRD diffractogram is typical for amorphous polymer showing large amorphous halo resulting from the lack of long range ordering in the material. Typically, PTh have tendency to form semicrystalline polymer having specific broad peak between 25° and 30°. The absence of crystalline phase in the polymer indicates incorporation of surfactant molecules in the spaces between PTh chains and decrease of their interchain interactions, known as main cause of close packing and crystallite formation of the polymer.

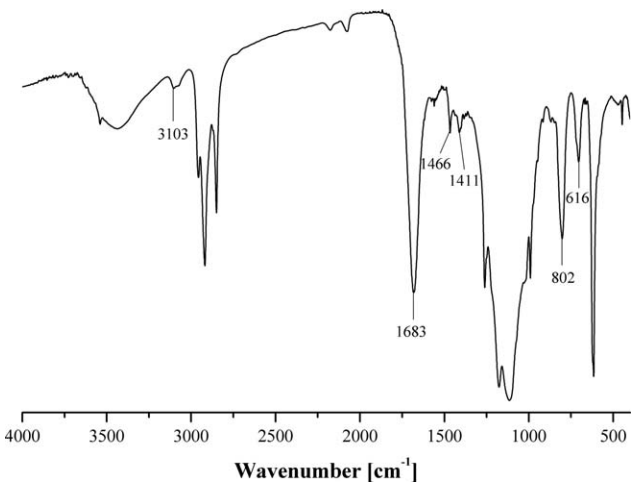

Figure 5. FTIR spectrum of polythiophene Polymer I.

Scanning Electron Microscopy (SEM)

The morphology of polymers synthesized during this study was tested by means of scanning electron microscopy. The SEM image of the polythiophene synthesized according to procedure I, shown in Figure 7(a), form the particles shaped in form of nanowires. Their edges were not uniform with a series of rounded protrusions occurring at each edge along their full length. The diameters are in the range 20 to 65 nm and lengths amounted to several micrometers. The product II has the form of spherical particles [Figure 7(b)] of diameters in the range 0.3 to 1 μm. Finally, the SEM image of product III presented the agglomerated assemblage of the small spheroidal grains of polymer [Figure 7(c)] with average particle diameter approximately 200 nm.

In course of this study, three different surfactant have been utilized to stabilize the reacting emulsion. The chain growing step of the polymerization took place inside the monomer swollen micelles of a surfactant. In this context, the micelles size and shape influence the morphology of the product. Typically, surfactant micelles have spherical shape, however, in certain conditions they can form rod-like structures. As it was found from SEM images of the product Polymer II and Polymer III synthesized using CTAB and DBSA, respectively, have spherical shape, which indicates that monomer swollen micelles have had the same shape. The difference in the product concerns the average polymer particle size and state of their aggregation. Polymer II synthesized in presence of CTAB, which is known to prevent particles aggregation via Derjaguin–Landau–Verwey–Overbeek (DLVO) mechanism. As it is seen from Figure 7(b), Polymer II is composed of nice isolated spheres. However Polymer III synthesized in presence of DBSA, have spherical particle of

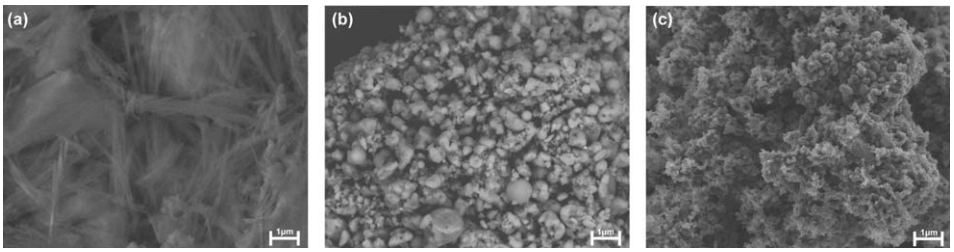

Figure 7. The SEM images of polythiophene obtained in different synthesis conditions (a) Polymer I, (b) Polymer II, and (c) Polymer III.

nanometric size aggregated in shapeless lumps. However, Polymer I synthesized in presence of SDS form the rod-like particles, which indicates that during chain growth stage of synthesis monomer swollen SDS micelles shift shape from typical for water solution spheroid into extended rod-like system. Similar findings have been reported in the literature for similar emulsion systems including different surfactants i.e., thiophene/SDS/$FeCl_3$ and thiophene/CTAB/$FeCl_3$ led to significantly different morphology of resulting polymer.[11] In the former case, polymer particles ware spherical, while in the latter polythiophene was in the form of plates. According to this, one can conclude that aside of the micelle features also polymerization initiator strongly influence polymer morphology.

Thermal Studies

There is relatively little literature reports concerning the thermal stability of PTh. In this context, it is difficult to discuss obtained results in the wider perspective. In this work, we have studied thermal properties of Polymer I by using thermogravimetric analysis (TGA). The respective thermogravimetry (TG) and differential thermal analysis (DTA) curves are shown in Figure 8 indicating that during the heating of the sample decomposition accompanied by significant mass loss starts about 190 °C. The weight loss 5%, determined from TGA curve, occurs at 220.41 °C, which is close to the value given in the literature for PTh synthesized by organometallic coupling.[35] According to the DTA plot, the highest rate of thermal degradation occurs in the temperature range from 240 to 440 °C. However at 600 °C, the total mass loss does not exceeds 20% of initial polymer mass.

To determine the phase transition occurring in the investigated polymer DSC analysis was carried out for two samples of PTh. The first was Polymer I synthesized in aqueous medium according to the procedure given in the Experimental section of this article. For the sake of comparison, the second sample consisted of PTh obtained by oxidative polymerization in chloroform according to the procedure analogue to the one described in our previous work.[36] The second polymer had one significant feature on the DSC thermogram (Figure 9) indicating glass transition temperature (T_g) at 147.75 °C. On the contrary, the Polymer I obtained via emulsion polymerization showed that on the DSC scan, four second-order phase transition regions occurring at 57.70 °C, 95.86 °C, 112.92 °C, and 137.58 °C. Observed behavior of Polymer I can be explained by the presence of the surfactants in the reaction mixture. Resulting polymer still contain little amount of surfactants which act as plasticizers. It is commonly known that increase of plasticizer content decrease the T_g of polymer. The presence of four such transitions can be understood in terms of formation of four major fractions of polymer having different degree of plasticization. The fact, that polymer obtained via emulsion polymerization include plasticizer can be an advantage in context of further processing of the material. In general, PTh obtained in organic solvents is unprocessable. The new polymer, however not chemically pure, can be potentially processed. The plasticizer incorporated in the polymer mass diminishes the intermolecular interaction between neighboring polythiophene chains.

Electrochemical Characterization of the Material

To characterize the electrochemical properties of this electroactive polymer, voltammetric studies have been carried out on specimens in form pellet pressed from polymer powder. Resulting cyclic voltammograms recorded at different scan rates are

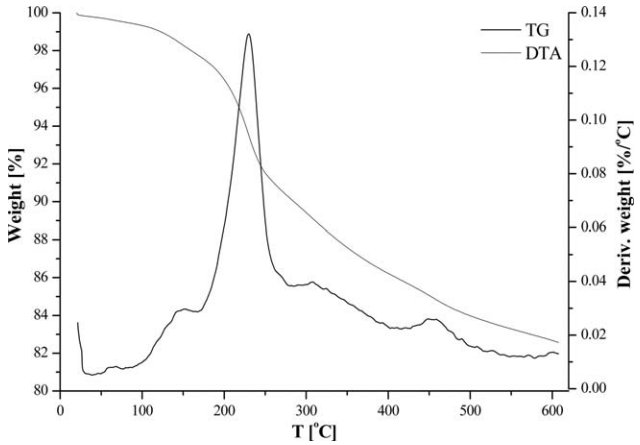

Figure 8. Thermogravimetric analysis of polythiophene Polymer I.

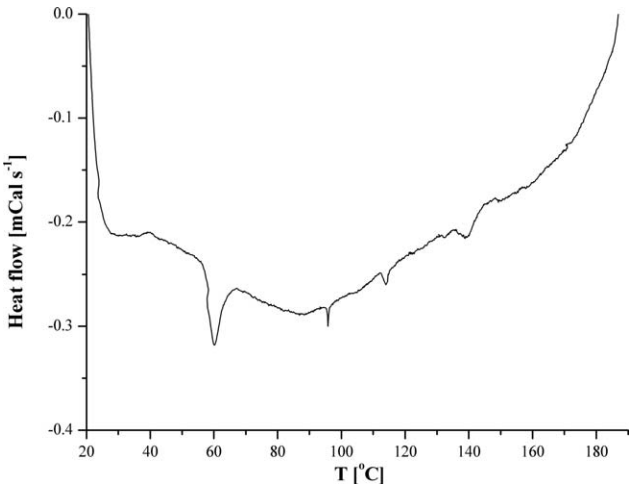

Figure 9. The thermogram of Polymer I DSC.

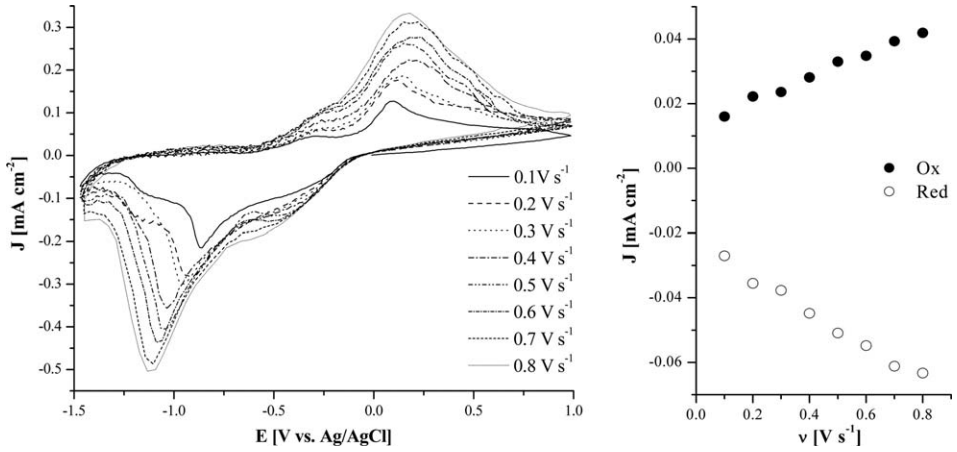

Figure 10. Electrochemical studies of Polymer I; (a) CV at different scan rates in monomer-free solution and (b) the plot of peak current vs. scan rate.

shown in Figure 10(a). The redox process of Polymer I is chemically irreversible. A single oxidation process and a single reduction process are observed. The anodic peak potential (oxidation) recorded in the range from 0.10 V to 0.18 V vs. Ag/AgCl and the cathodic peak potential (reduction) registered in the range from −0.86 V to −1.3 V vs. Ag/AgCl. The study of the specific peak currents revealed linear relationship between peak current and scan rate in case of anodic as well as cathodic peak [Figure 10(b)]. These linear plots show that the studied process is not controlled by diffusion.

Current–Voltage Characteristics of the Polymers in Native (Nondoped) State

The collected data clearly indicate that the polythiophene covered with gold electrodes complies with Ohm's law. The resulting specimen show linear relationship of current and applied voltage, at three selected temperatures 298, 308, and 318 K (Figure 11). The specific volume resistance of test compound increase with temperature, which is significant for semiconductors. Table II contain the data of dc-conductivity (σ_{dc}) for PTh—obtained by three methods—recorded for three respective temperatures.

The conductivity of substance (σ_{298}, σ_{308}, and σ_{318}) at different temperatures (i.e., 298, 308, and 318 K, respectively) was calculated using the following equation:

$$\sigma_{dc} = \frac{I \times d}{V \times s}$$

where I is the current (A), V is the voltage (V), d is the thickness of pills (m), and s is the surface of electrode (m^2).

Activation Energy of Electric Conductivity of the Materials in Native (Nondoped) State

The results of $\ln\sigma = f(1/T)$ dependency measurement for PTh shown in Figure 12 allow for a classification of the product to the group of semiconductors. The plot is linear and the temperature dependence of σ_{dc} follows Arrhenius-type behavior. Thus, the activation energy of the polythiophene was calculated by the following formula:

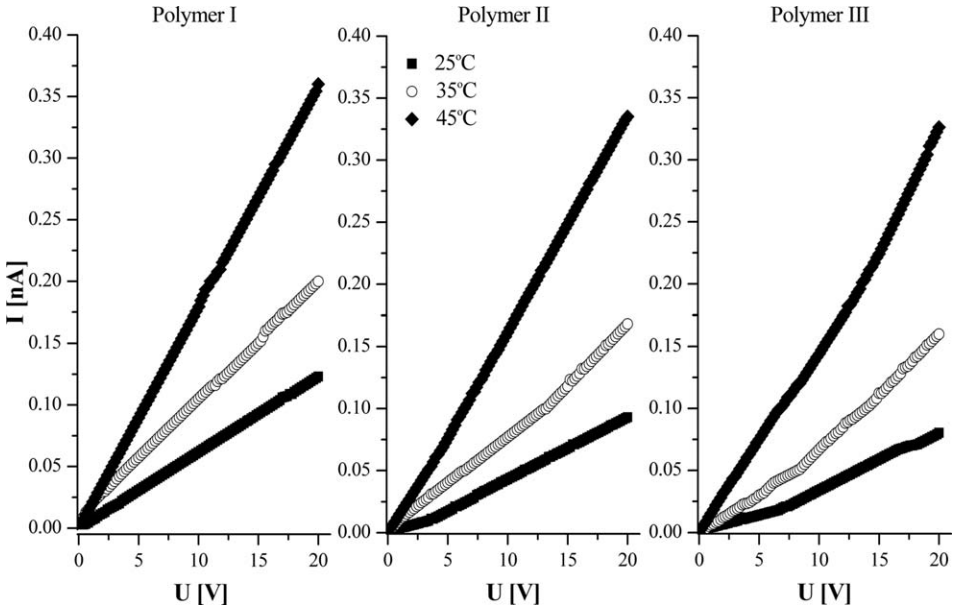

Figure 11. Current–voltage characteristics of PTh pressed powder samples of (a) Polymer I, (b) Polymer II, and (c) Polymer III.

Table II. Electrochemical Properties of PTh

Property	Polymer I	Polymer II	Polymer III
E_a (eV)	0.896 ± 0.003	0.885 ± 0.002	0.892 ± 0.003
σ_0 (nS m^{-1})	1006 ± 3	1092 ± 3	1247 ± 4
σ_{298} (nS m^{-1})	0.401 ± 0.002	0.316 ± 0.001	0.247 ± 0.001
σ_{308} (nS m^{-1})	0.622 ± 0.003	0.527 ± 0.002	0.523 ± 0.002
σ_{318} (nS m^{-1})	1.162 ± 0.006	1.105 ± 0.005	1.021 ± 0.005
$\sigma_{t=0}$ (nS m^{-1})	5.407 ± 0.030	2.471 ± 0.020	2.007 ± 0.010
$\sigma_{t=1h}$ (nS m^{-1})	546 ± 2	501 ± 2	402 ± 1

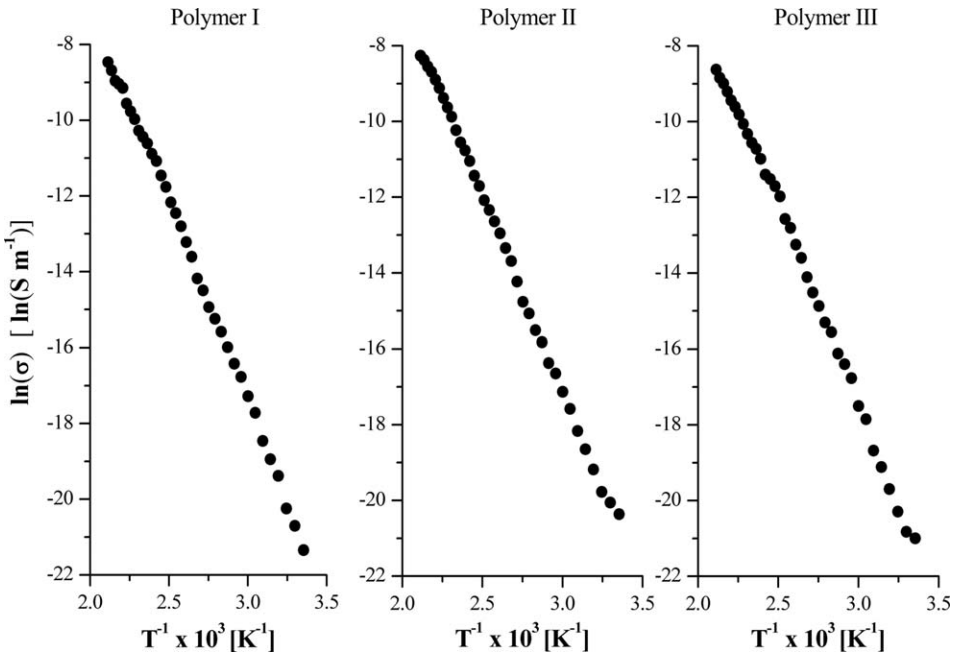

Figure 12. Temperature dependence of electronic conductivity of PTh (a) Polymer I, (b) Polymer II, and (c) Polymer III.

$$\ln_{dc} = \ln_0 - \frac{E_g}{2k_B T}$$

where σ_0 is the conductivity limit (S m^{-1}), E_g is the size of energy gap, $E_g = 2E_a$ (eV), E_a is the activation energy (eV), k_B is the Boltzmann constant (8.617 × 10^{-5} eV K^{-1}), and T is the temperature (K).

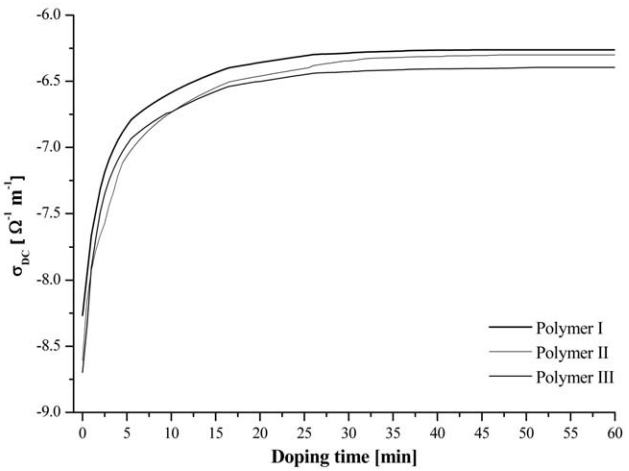

Figure 13. Iodine doping kinetics of PTh.

The value of the activation energy obtained for all three types of polythiophene together with preexponential term σ_0 are given in Table II.

Doping Processes

The kinetics of the iodine doping was investigated, by means of the current change as a function of the time during exposure to iodine fumes of constant partial pressure. Polymer was prepared in form of polythiophene pellet with gold contacts. The data collected during the investigation are presented in plot of log $(\sigma) = f(t)$ (Figure 13). The conductivity of the polymer increase in a logarithmic manner with exposition time. In the first stage, dc-conductivity grows sharply indicating the formation of unpaired spin charge carriers (positive polarons). In the second stage, the curve approaching certain limiting value, which is significant for the formation of bications. Thus, PTh shows a specific state of saturation with dopant vapor, beyond which dc-conductivity increases slightly ($t \approx 30$ min). Approximate number of charge carriers generated during the iodine

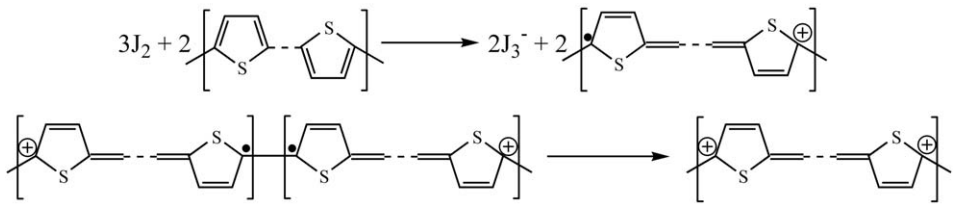

Figure 14. The scheme of iodine doping process.

doping process for Polymer I, II, and III reaches 5×10^{17}, 3×10^{17}, and 2×10^{17}, respectively.

Changes in dc-conductivity values prior to the process ($\sigma_{t=0}$) and after one hour exposure ($\sigma_{t=1\ h}$) are presented in the Table II. The dc-conductivity value rise by two orders of magnitude. The polythiophene becomes a p-type semiconductor. The mechanism of the iodine doping is shown in Figure 14.

CONCLUSIONS

In summary, the emulsion polymerization of thiophene is an effective method for preparing conductive polymers. The polythiophene was successfully received using the three systems of initiator–surfactant. The obtained results clearly indicate that the use of potassium peroxydisulfate (KPS) as initiator and sodium dodecyl sulfate (SDS) as the surfactant gives the best product yields. The properties of PTh have been tested and the mechanism for the polymerization has been proposed. Careful analysis of the vibration spectrum of polymer proves that the polythiophene was obtained with reasonable purity, and it contain some amount of surfactant molecules responsible for amorphous morphology of the material ascertained by XRD analysis.

In the analyzed cases, the morphological transformation processes of polythiophene are observed. The products have the form of wires or grains with varying sizes.

The Polymer I shows typical for polythiophene thermal decomposition temperature. The DSC scan revealed that the remains of the surfactant used during synthesis act as plasticizer decreasing intermolecular interactions between the PTh chains, which can make the polymer potentially processable.

All polythiophenes obtained in the course of this study have good electrical properties. The collected information clearly indicates that the compound complies with Ohm's law. The data allow for a classification of the product to the group of semiconductors. Iodine doping of the polymer substantially increase the dc-conductivity clearly indicating p-doping. It has been observed that the conductivity of the polymers changes in a logarithmic manner, up to attaining certain limiting value. The electrochemical properties of the products obtained by three different methods are similar.

The emulsion polymerization of polythiophene described in this review is desirable from the viewpoint of mass production, because it is environment-friendly chemical process, clean, and safe.

ACKNOWLEDGMENTS

This work was financially supported by research grant ZB 287 from the Department of Chemistry, UMK in Toruń.

REFERENCES

1. Gurunathan, K.; Vadivel Murugan, A.; Marimuthu, R.; Mulik, U. P.; Amalnerkar, D. P. *Mater. Chem. Phys.* **1999**, *61*, 173.
2. Zhang, H.; Hu, L.; Tu, J.; Jiao, S. *Electrochim. Acta* **2014**, *120*, 122.
3. Li, B.; Santhanam, S.; Schultz, L.; Jeffries-El, M.; Iovu, M. C.; Sauvé, G.; Cooper, J.; Zhang, R.; Revelli, J. C.; Kusne, A. G.; Snyder, J. L.; Kowalewski, T.; Weiss, L. E.; McCullough, R. D.; Fedder, G. K.; Lambeth, D. N. *Sens. Actuator B Chem.* **2007**, *123*, 651.
4. Liao, F.; Toney, M. F.; Subramanian, V. *Sens. Actuator B Chem.* **2010**, *148*, 74.
5. Bizid, S.; Mlika, R.; Haj Said, A.; Chemli, M.; Korri Youssoufi, H. *Sens. Actuator B Chem.* **2016**, *226*, 370.
6. Hou, X.; He, J. *Eur. Polym. J.* **2015**, *70*, 157.
7. Bunz, U. H. F. *Chem. Rev.* **2000**, *100*, 1605.
8. An, W.; Zhang, J.; Zhu, T.; Gao, N. *Ren. Energy* **2016**, *86*, 633.
9. Syrový, T.; Kuberský, P.; Sapurina, I.; Pretl, S.; Bober, P.; Syrová, L.; Hamáček, A.; Stejskal, J. *Sens. Actuator B Chem.* **2016**, *225*, 510.
10. Scherf, U.; List, E. J. W. *Adv. Mater.* **2002**, *14*, 477.
11. Senthilkumar, B.; Thenamirtham, P.; Kalai Selvan, R. *Appl. Surf. Sci.* **2011**, *257*, 9063.
12. El-Maghraby, A. A.; Abou-Elenien, G. M.; El-Abdallah, G. M. *Synth. Met.* **2010**, *160*, 1335.
13. del Valle, M. A.; Gacituaa, M.; Diaz, F. R.; Armijo, F.; Soto, J. P. *Electrochim. Acta* **2012**, *71*, 277.
14. Liu, R. C.; Liu, Z. P. *Chinese Sci. Bull.* **2009**, *54*, 2028.
15. Lee, S. J.; Lee, J. M.; Cheong, I. W.; Lee, H.; Kim, J. H. *J. Polym. Sci. A: Polym. Chem.* **2008**, *46*, 2097.
16. Ai, L.; Liu, Y.; Zhang, X. Y.; Ouyang, X. H.; Ge, Z. Y. *Synth. Met.* **2014**, *191*, 41.
17. Lee, J. M.; Lee, S. J.; Jung, Y. J.; Kim, J. H. *Curr. Appl. Phys.* **2008**, *8*, 659.
18. Gök, A.; Omastová, M.; Yavuz, A. G. *Synth. Met.* **2007**, *157*, 23.
19. Wang, Z.; Wang, Y.; Xu, D.; Kong, E. S. W.; Zhang, Y. *Synth. Met.* **2010**, *160*, 921.

20. Dai, L.; Xu, Y.; Gal, J. Y.; Lu, X.; Wu, H. *Polym. Int.* **2002**, *51*, 547.
21. Yeh, J. M.; Kuo, T. H.; Huang, H. J.; Chang, K. C.; Chang, M. Y.; Yang, J. C. *Eur. Polym. J.* **2007**, *43*, 1624.
22. Kane, M.; Krafcik, K. *Synth. Met.* **2013**, *181*, 129.
23. Martínez, M. V.; Bongiovanni Abel, S.; Rivero, R.; Miras, M. C.; Rivarola, C. R.; Barbero, C. A. *Polymer* **2015**, *78*, 94.
24. Gök, A.; Sari, B.; Talu, M. *J. Appl. Polym. Sci.* **2005**, *98*, 2048.
25. Choi, J. W.; Han, M. G.; Kim, S. Y.; Oh, S. G.; Im, S. S. *Synth. Met.* **2004**, *141*, 293.
26. Wu, C. H.; Don, T. M.; Chiu, W. Y. *Polymer* **2011**, *52*, 1375.
27. Wu, C. H.; Chiu, W. Y.; Don, T. M. *Polymer* **2012**, *53*, 1086.
28. Yoon, S. J.; Chun, H.; Lee, M. S.; Kim, N. *Synth. Met.* **2009**, *159*, 518.
29. Jung, Y. J.; Lee, S. M.; Sankaraiah, S.; Cheong, I. W.; Choi, S. W.; Kim, J. H. *Macromol. Res.* **2011**, *19*, 1114.
30. Lee, S. J.; Lee, J. M.; Cho, H. Z.; Koh, W. G.; Cheong, I. W.; Kim, J. H. *Macromolecules* **2010**, *43*, 2484.
31. Ye, Q.; Wang, C.; Wang, D.; Sun, G.; Xu, X. *J. Zhejiang Univ. Sci. B* **2006**, *7*, 404.
32. Aksüt, A.; Bayramoğlu, G. *Commun. Fac. Sci. Univ. Ank. Series B* **1994**, *40*, 83.
33. Wei, Y.; Chan, C. C.; Tian, J.; Jang, G. W.; Hsueh, K. F. *Chem. Mater.* **1991**, *3*, 888.
34. Kelkar, D. S.; Chourasia, A. B. *Indian J. Phys.* **2012**, *86*, 101.
35. Nowaczyk, J.; Blockhuys, F.; Czerwiński, W. *Mater. Chem. Phys.* **2012**, *132*, 823.
36. Toshima, N.; Hara, S. *Prog. Polym. Sci.* **1995**, *20*, 155.